# Molecular Electrostatic Potentials and Hydrogen Bonding in α-, β-, and γ-Cyclodextrins

**Rahul V. Pinjari, Kaustubh A. Joshi, and Shridhar P. Gejji***

*Department of Chemistry, University of Pune, Ganeshkhind, Pune 411007, India*

*Received: August 10, 2006; In Final Form: September 29, 2006*

Cyclodextrins (CDs) are cyclic oligomers of glucose having the toroid of sugars elaborating a central cavity of varying size depending on the number of glucoses. The central hydrophobic cavity of CD shows a binding affinity toward different guest molecules, which include small substituted benzenes to long chain surfactant molecules leading to a variety of inclusion complexes when the size and shape complimentarity of host and guest are compatible. Further, interaction of guest molecules with the outer surface of α-CD has also been observed. Primarily it is the electrostatic interactions that essentially constitute a driving force for the formation of inclusion complexes. To gain insights for these interactions, the electronic structure and the molecular electrostatic potentials in α-, β-, and γ-CDs are derived using the hybrid density functional theory employing the three-parameter exchange correlation functional due to Becke, Lee, Yang, and Parr (B3LYP). The present work demonstrates how the topography of the molecular electrostatic potential (MESP) provides a measure of the cavity dimensions and understanding of the hydrogen-bonded interactions involving primary and secondary hydroxyl groups. In α-CD, hydrogen-bonded interactions between primary −OH groups engender a "cone-like" structure, while in β- or γ-CD the interactions from the primary −OH with ether oxygen in glucose ring facilitates a "barrel-like" structure. Further, the strength of hydrogen-bonded interactions of primary −OH groups follows the rank order α-CD > β-CD > γ-CD, while the secondary hydrogen-bonded interactions exhibit a reverse trend. Thus weak hydrogen-bonded interactions prevalent in γ-CD manifest in shallow MESP minima near hydroxyl oxygens compared to those in α- or β-CD. Furthermore, electrostatic potential topography reveals that the guest molecule tends to penetrate inside the cavity forming the inclusion complex in β- or γ-CD.

## Introduction

Cyclodextrin (CD) or cycloamylose (CA) represents a family of macrocyclic oligosaccharides consisting of six (α-CD), seven (β-CD), or eight (γ-CD) D-glucose units linked by α(1→4) glycosidic bonds. The specific coupling of glucose monomers engenders a rigid conical molecular structure with a hydrophilic exterior and hollow hydrophobic interior of a specific volume. This internal cavity is capable of accommodating a wide range of guest molecules, ranging from polar compounds such as alcohols, acids, amines, and small inorganic anions to nonpolar aliphatic and aromatic hydrocarbons.[1] The inside cavity of appropriate dimension is conducive to binding to various guest molecules to form inclusion complexes in aqueous solution[2] which find potential applications in pharmaceutical science,[3] catalysis,[4] and separation technology,[5−7] and in affinity chromatography[8,9] as chiral discriminators against optically active molecules. Owing to multifunctional characteristics and bioadaptability, α-, β-, and γ-CDs have been explored in biochemistry and drug research. Recent investigations have shown that inclusion complexes of CDs can act as carriers for biologically active substances.[10−15] The principal advantages of natural CDs as drug carriers may be traced back to their well-defined chemical structure, offering a multitude of potential sites for chemical modification, availability of different cavity sizes, low toxicity and low pharmacological activity, and protection of the guest molecule from biodegradation.[16−18] Inclusion complexes of CDs serve as ideal models mimicking enzyme−substrate interactions.[19] The α-, β-, and γ-cyclic oligomers are useful for phase transfer in catalysis[20] and have further been explored as building blocks in supramolecular structures and functional units[21] and in asymmetric catalysis.[22]

To understand host−guest interactions, the structural elucidation of CDs and their inclusion complexes in the liquid and solid states are studied using NMR spectroscopy.[23] The crystal structure of CD hydrates and cyclodextrin inclusion complexes have been determined by X-ray and neutron diffraction.[24−29] The effect of alkali metal chlorides on the self-association of decanoic acid and its inclusion in β-CD has been studied with the help of $^1$H NMR spectroscopy.[30] The solid-state inclusion complex of β-CD and 2-phenoxyethanol and its properties have been characterized[31] for different humidities using powder X-ray diffraction (PXRD), thermogravimetry, Fourier transform (FT) Raman spectroscopy, and $^{13}$C cross-polarization (CP) MAS NMR. In contrast, the synthesis of CD hydrates and complexes with no guest molecule inside the cavity, for example, α-CD complexes of benzene and iodoanilide trihydrate, are also reported in the literature.[24,32,33] The binding constants of a variety of guests with cyclodextrins in water are reported in the literature.[34] Association binding constants of phenol and CD[35] have been obtained by near-infrared spectroscopic measurements. It has also been observed that phenol and CD interaction in the ionic liquids turns out to be external adsorption.

Thermodynamic studies on cyclodextrin complexation of aromatic guests in water and urea−water mixtures have also been reported.[36] Along with these experiments theoretical methods,[37] including molecular mechanics (MM),[38] have been useful to a certain degree to understand the host−guest

* To whom correspondence should be addressed. Fax: +91-20-25691728. E-mail:spgejji@chem.unipune.ernet.in.

10.1021/jp065169z CCC: $33.50 
Published on Web 11/11/2006

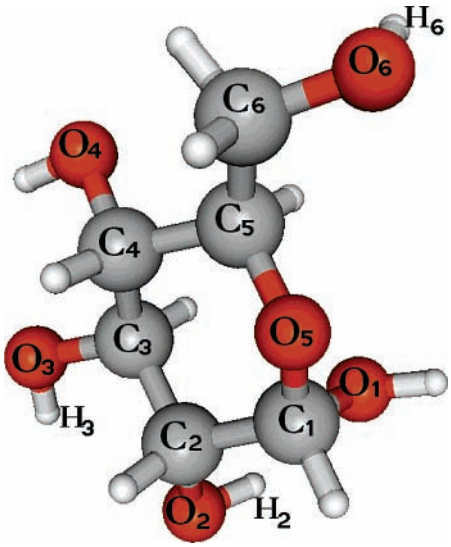


**Figure 1.** Atomic numbering scheme in glucose.

interactions in CD complexes. Accordingly, the inclusion complexes of $\beta$-cyclodextrin with aliphatic alcohols are investigated using empirical force fields.[39] Calculated vibrational frequencies are subsequently used to estimate the Gibbs free energy and related thermodynamic parameters. Thermodynamic and NMR studies[40] have shown that the reactions of α- and $\beta$-CDs with acids, aliphatic amines, and cyclic alcohols can be qualitatively understood in terms of van der Waals forces and hydrophobic effect. It has been shown further that the standard Gibbs free energy correlates well with the structural features of ligands. Molecular dynamics (MD) simulations have widely been used recently to derive the thermodynamic parameters of the CD complexation.[41] Estrada and co-workers[42] have utilized the simulations on the complexes of α- and $\beta$-CDs with substituted benzene derivatives and obtained the quantitative structure−property relations. MD simulations on $\beta$-CD hydration[43] have shown that hydrophobicity dominates inside the cavity, whereas at the top and bottom interactions with water are mostly hydrophilic in nature.

Crystallographic data for the spontaneous hydration process of a CD crystal in wet atmosphere concur with the calculated results.[43] Complexation with organic and inorganic guest molecules have also been studied using semiempirical quantum chemical calculations. Calculations based on the Parametric Method-3 (PM3) have been carried out to predict the structure of the α-CD and 4-fluorophenol complex.[44] These calculations have shown that the −OH group of the guest directs toward the primary hydroxyls of α-CD in solid state. It has also been remarked that solvation has a profound influence and may reverse the orientation of the guest. Lipkowitz,[37] however, has questioned the use of semiempirical methods to yield the structures of cyclodextrins. Semiempirical quantum chemical methods have attained some success; however, they have failed to account for weak intermolecular interactions.[45] Recently the Hartree−Fock and second-order Møller−Plesset (MP2) theories have been utilized to characterize the structure and normal vibrations of substrate in the inclusion complex of $CH_3HgCl$ and α-CD.[46] Thus, explicit inclusion of water molecules favor, the inclusion with the guest $CH_3HgCl$ orienting *perpendicular* to the CD ring. On the contrary, the structure with the guest orienting *parallel* to the ring has been observed experimentally. Single-point hybrid density functional calculations on the structure consisting of two water molecules inside the cavity and four outside the cavity are used to obtain the thermodynamic

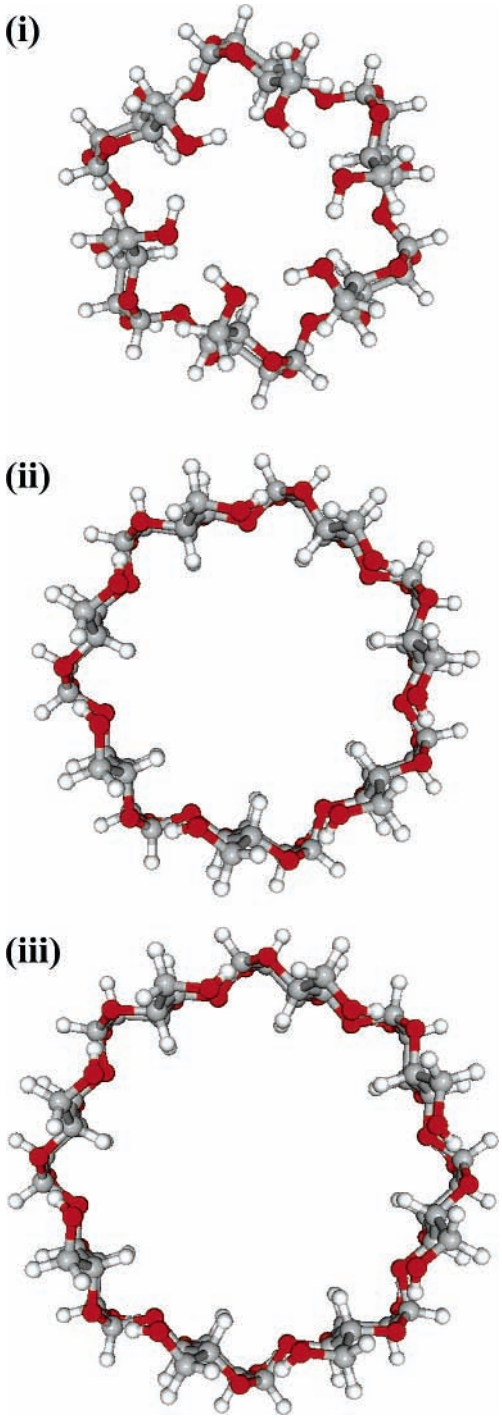


**Figure 2.** B3LYP optimized structures of (i) α-CD, (ii) $\beta$-CD, and (iii) $\gamma$-CD (top view).

parameters, viz., entropy, enthalpy, and Gibbs free energy of hydration of the α-CD hexahydrate,[47] which compare well with those from experiment. Quantum chemical calculations at the electron correlation level of theory could not be utilized for the optimization of such large systems.

Very recently, the molecular structure, stabilization energy, and thermodynamic properties of the interaction of α-CD dimers[48] (head to head, tail to tail, and head to tail) with water clusters were derived successfully using density functional calculations with the PM3 optimized geometries. From these calculations it has been shown that the inter-α-CD hydrogen-bonded interactions render stability to the dimeric structures and no water tetramer was found between the two α-CD subunits

**TABLE 1: B3LYP Optimized Geometric Parameters (Bond Distances in Å and Bond Angles in deg) in α-, *β*-, and *γ*-Cyclodextrins**

| | α-CD | | *β*-CD | | *γ*-CD | |
|---|---|---|---|---|---|---|
| | B3LYP | expt | B3LYP | expt | B3LYP | expt |
| $C_1O_4'$ | 1.409 | 1.416 | 1.410 | 1.419 | 1.411 | 1.421 |
| $C_1O_5$ | 1.412 | 1.418 | 1.420 | 1.414 | 1.419 | 1.406 |
| $C_1C_2$ | 1.534 | 1.533 | 1.531 | 1.524 | 1.532 | 1.525 |
| $C_2C_3$ | 1.532 | 1.510 | 1.529 | 1.527 | 1.529 | 1.527 |
| $C_2O_2$ | 1.415 | 1.430 | 1.411 | 1.439 | 1.410 | 1.425 |
| $C_3C_4$ | 1.527 | 1.522 | 1.524 | 1.485 | 1.523 | 1.555 |
| $C_3O_3$ | 1.423 | 1.440 | 1.425 | 1.439 | 1.424 | 1.436 |
| $C_4C_5$ | 1.541 | 1.535 | 1.543 | 1.536 | 1.542 | 1.526 |
| $C_4O_4$ | 1.429 | 1.441 | 1.432 | 1.453 | 1.432 | 1.440 |
| $C_5C_6$ | 1.534 | 1.516 | 1.539 | 1.527 | 1.539 | 1.512 |
| $C_5O_5$ | 1.444 | 1.445 | 1.455 | 1.450 | 1.455 | 1.458 |
| $C_6O_6$ | 1.427 | 1.440 | 1.408 | 1.392 | 1.408 | 1.431 |
| $C_1C_4$ | 2.898 | 2.878 | 2.906 | 2.852 | 2.908 | 2.888 |
| $C_1C_4'$ | 2.463 | 2.454 | 2.461 | 2.467 | 2.451 | 2.436 |
| $O_2O_3$ | 2.894 | 2.910 | 2.809 | 2.895 | 2.794 | 2.887 |
| $O_2O_3'$ | 3.154 | 2.981 | 2.830 | 2.858 | 2.800 | 2.823 |
| $O_4O_4'$ | 4.370 | 4.235 | 4.444 | 4.378 | 4.551 | 4.501 |
| $O_5O_6$ | 3.187 | 2.870 | 3.644 | 2.823 | 3.644 | 2.828 |
| $O_4O_6$ | 4.036 | 3.645 | 3.092 | 3.853 | 3.073 | 3.847 |
| $O_4'O_5$ | 2.337 | 2.335 | 2.332 | 2.331 | 2.333 | 2.328 |
| $C_4'O_4'C_1$ | 120.4 | 118.4 | 120.0 | 118.3 | 119.1 | 116.8 |
| $O_4'C_1O_5$ | 111.9 | 111.0 | 111.0 | 110.8 | 111.1 | 111.0 |
| $O_4'C_1C_2$ | 106.6 | 107.6 | 109.1 | 108.1 | 109.6 | 108.7 |
| $C_1C_2C_3$ | 109.5 | 110.2 | 109.2 | 110.0 | 109.6 | 110.7 |
| $C_1C_2O_2$ | 112.7 | 108.1 | 114.3 | 109.4 | 114.5 | 110.3 |
| $C_1O_5C_5$ | 114.2 | 114.0 | 116.1 | 114.0 | 116.7 | 114.5 |
| $C_2C_3C_4$ | 111.9 | 111.0 | 110.7 | 109.1 | 110.0 | 109.8 |
| $C_2C_1O_5$ | 110.5 | 109.2 | 109.5 | 110.2 | 109.8 | 110.9 |
| $O_2C_2C_3$ | 110.9 | 110.6 | 110.8 | 110.9 | 110.9 | 110.5 |
| $C_2C_3O_3$ | 111.2 | 109.0 | 109.7 | 109.8 | 109.4 | 109.4 |
| $C_3C_4C_5$ | 109.6 | 112.0 | 110.3 | 111.6 | 109.7 | 109.7 |
| $C_3C_4O_4$ | 105.3 | 106.0 | 106.9 | 106.9 | 107.7 | 106.6 |
| $O_3C_3C_4$ | 108.4 | 108.8 | 109.0 | 110.0 | 109.2 | 109.4 |
| $C_4C_5C_6$ | 116.4 | 113.3 | 115.3 | 114.0 | 115.5 | 114.1 |
| $C_4C_5O_5$ | 108.8 | 109.2 | 109.0 | 108.1 | 108.6 | 107.5 |
| $O_4C_4C_5$ | 111.1 | 108.1 | 111.4 | 108.0 | 111.9 | 109.7 |
| $O_5C_5C_6$ | 106.9 | 106.1 | 104.5 | 105.5 | 104.3 | 105.8 |
| $C_5C_6O_6$ | 111.7 | 112.5 | 113.6 | 110.8 | 113.7 | 110.3 |
| $O_4O_4'O_4''$ | 120.0 | 119.9 | 128.6 | 128.3 | 135.1 | 134.9 |
| $C_5C_6O_6H$ | 108.5 | | 73.4 | | 74.9 | |
| $HC_5C_6O_6$ | −22.5 | | 49.8 | | 51.2 | |
| $C_5O_5C_1O_4'$ | 56.4 | | 60.2 | | 63.1 | |
| $O_5C_1O_4'C_4'$ | 98.9 | | 113.6 | | 114.0 | |
| $O_5C_1C_2O_2$ | 178.5 | | −178.1 | | −179.1 | |
| $C_2O_2HO_3'$ | 109.3 | | 111.9 | | 112.8 | |
| $C_3O_3HO_2$ | 20.4 | | 19.2 | | 19.4 | |
| $C_3C_4O_4C_1''$ | 135.6 | | 125.1 | | 124.5 | |
| $C_4C_5C_6O_6$ | −143.1 | | −73.5 | | −72.6 | |

**TABLE 2: B3LYP Optimized Average Hydrogen-Bonding Distances (in Å) in α-, *β*-, and *γ*-Cyclodextrins**

| | α-CD | *β*-CD | *γ*-CD |
|---|---|---|---|
| $O_6-H\cdots O_6$ | 1.804 | | |
| $O_6-H\cdots O_5$ | | 1.920 | 1.922 |
| $O_3-H\cdots O_2$ | 2.424 | 2.290 | 2.270 |
| $O_2-H\cdots O_3$ | 2.243 | 1.882 | 1.854 |

in the lowest minimum structure. Thus, binding of water molecules to the α-CD dimer or their inclusion complexes in aqueous media has to be accounted for in the theoretical calculations. It should further be remarked here that electrostatic interactions constitute an important driving force in cyclodextrin complexation.[49] Alternatively, electronic repulsion between frontier orbitals of the host and guest has been conjectured to be a driving force[42] in the α-CD−benzene derivative complex. The benzene ring is placed outside the cavity in these complexes. Complexation of *β*-CD with benzene derivatives, on the other hand, is controlled by topological and topographic parameters indicating the relevance of the van der Waals and hydrophobic interactions.[42] In *β*-CD complexes the guest penetrates deeply into the hydrophobic cavity of the host. Inclusion complexes of *γ*-CD, on the contrary, are less well studied. A few reports where steady-state fluorescence and calculations based on molecular mechanics have been used to determine the stoichiometry and binding constants of the inclusion complexes of 2-methylnaphthoate and *γ*-CD have appeared in the literature.[50] Complete penetration of the guest has been observed in both *β*- and *γ*-CDs. Time-resolved emission spectra measurements have been carried out to understand the influence of cavity size on the excited-state dynamics of methyl 4-(dimethylamino)-benzoate and cyclodextrin complexes.[51] In pursuance of understanding of underlying differences in the complexation at the molecular level, we derive the electronic structure and molecular electrostatic potential (MESP) of α-, *β*- and *γ*-CDs utilizing the hybrid density functional calculations. The computational method employed for this study has been outlined below.

**TABLE 3: MESP Minima (in kJ mol$^{-1}$) in α-, *β*-, and *γ*-Cyclodextrins[a]**

| | α-CD | *β*-CD | *γ*-CD |
|---|---|---|---|
| $w_1$ | −59.5 | −235.2 | −234.3 |
| $w_2$ | −58.5 | −235.5 | −234.1 |
| $w_3$ | −56.3 | −235.6 | −234.2 |
| $w_4$ | −60.3 | −234.9 | −233.6 |
| $w_5$ | −57.3 | −235.1 | −234.3 |
| $w_6$ | −56.6 | −235.4 | −233.9 |
| $w_7$ | | −235.2 | −234.0 |
| $w_8$ | | | −233.8 |
| $x_1$ | −76.8 | −88.3 | −92.0 |
| $x_2$ | −76.9 | −88.5 | −92.1 |
| $x_3$ | −76.9 | −88.4 | −91.9 |
| $x_4$ | −76.5 | −88.4 | −91.9 |
| $x_5$ | −76.3 | −88.5 | −91.9 |
| $x_6$ | −76.3 | −88.9 | −91.9 |
| $x_7$ | | −88.3 | −91.9 |
| $x_8$ | | | −91.9 |
| $y_1$ | −184.8 | −176.1 | −174.9 |
| $y_2$ | −184.3 | −176.2 | −174.9 |
| $y_3$ | −183.9 | −176.2 | −174.9 |
| $y_4$ | −183.9 | −176.2 | −174.7 |
| $y_5$ | −184.0 | −176.4 | −174.7 |
| $y_6$ | −183.8 | −176.3 | −174.7 |
| $y_7$ | | −176.2 | −174.8 |
| $y_8$ | | | −174.7 |
| $z_1$ | −146.5 | −117.3 | −111.3 |
| $z_2$ | −146.4 | −117.4 | −111.5 |
| $z_3$ | −146.0 | −117.2 | −111.0 |
| $z_4$ | −146.6 | −117.1 | −111.3 |
| $z_5$ | −146.7 | −117.7 | −111.3 |
| $z_6$ | −144.9 | −117.6 | −111.3 |
| $z_7$ | | −117.2 | −110.8 |
| $z_8$ | | | −111.5 |

[a] Critical points near $O_6$ (primary hydroxyl group), $O_4$ (glycosidic linkage), and $O_2$ and $O_3$ (secondary hydroxyl groups) are denoted by "w", "x", "y", and "z", respectively. See text for details.

## Computational Method

Conformers of α-, *β*-, and *γ*-CDs exhibiting different types of hydrogen-bonded interactions from the primary hydroxyl groups interacting with either primary hydroxyl groups or ring oxygens of adjacent glucoses were considered. These conformers possess the clockwise hydrogen-bonding network in the upper rim and the counterclockwise hydrogen-bonding patterns in the lower rim. Geometric optimizations were carried out using the

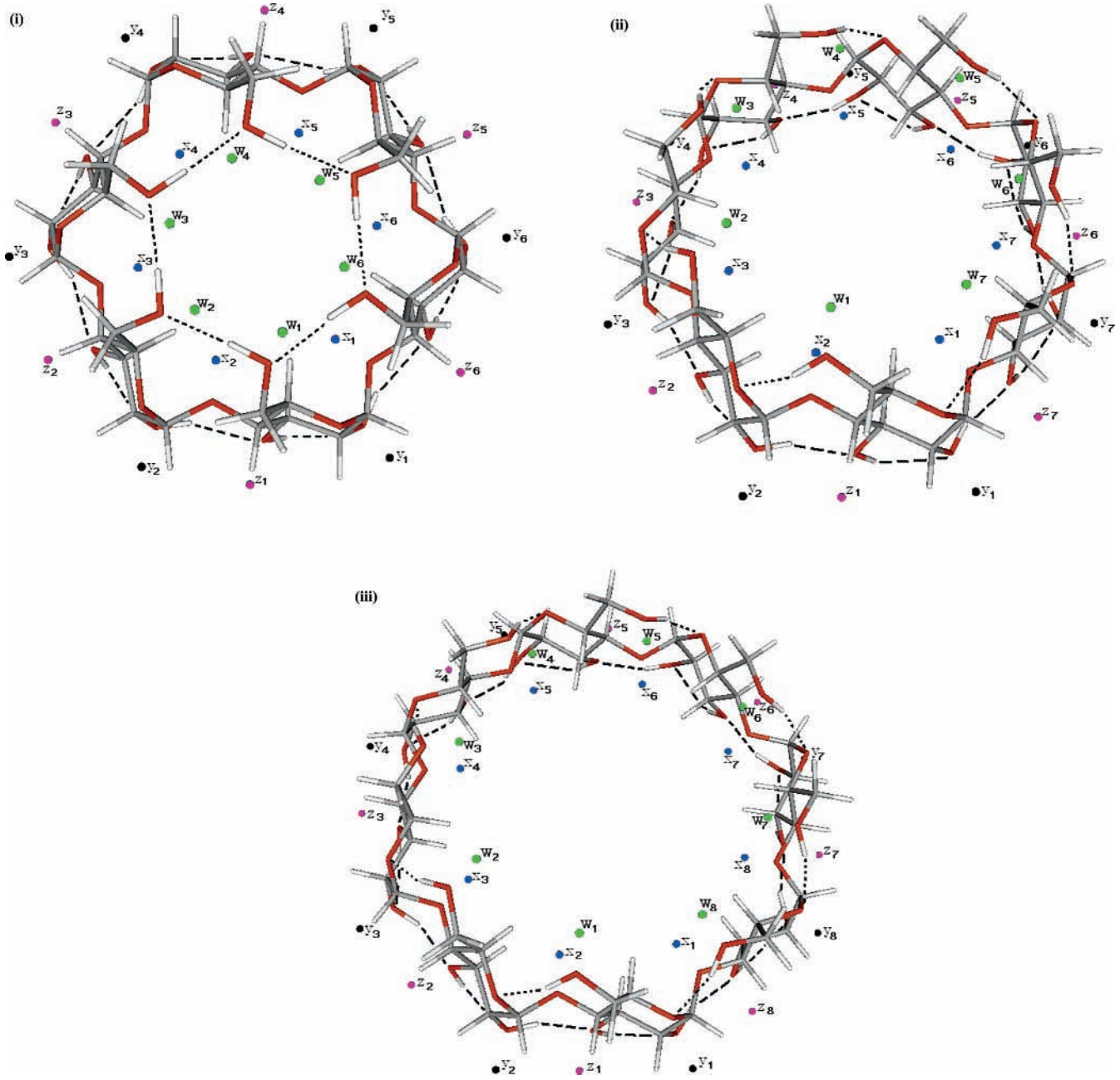


**Figure 3.** Hydrogen bonding and MESP minima in (i) α-CD, (ii) *β*-CD, and (iii) *γ*-CD.

semiempirical PM3 calculations. The lowest energy conformers thus obtained were subjected subsequently to optimizations using the density functional theory incorporating the B3LYP correlation functional.[52,53] The Gaussian 03 program[54] was used for all these geometric optimizations. The internally stored 6-31G-(d,p) basis set was employed. The MESP, $V(\mathbf{r})$, is given by the classical expression[55]

$$V(\mathbf{r}) = \sum_{A=1}^{N} \frac{Z_A}{|\mathbf{r} - \mathbf{R}_A|} - \int \frac{\rho(\mathbf{r}')\, \mathrm{d}^3\mathbf{r}'}{|\mathbf{r} - \mathbf{r}'|} \qquad (1)$$

In eq 1 $N$ is the total number of nuclei in the molecule and $Z_A$ defines the charge of the nucleus located at $\mathbf{R}_A$; $\rho(\mathbf{r})$ is the electron density. The two terms above refer to the bare nuclear potential and the electronic contributions, respectively. The balance of these two terms brings about the effective localization of electron-rich regions in the molecular system. The MESP topography is then mapped by examining the eigenvalues of the Hessian matrix at the point where the gradient $V(\mathbf{r})$ vanishes; the MESP critical points (CPs) were thereby located. A Fortran package UNIVIS-2000[56] was used for visualization of the MESP topography. It is customary to characterize[57] the CPs in terms of an ordered pair $(R,\sigma)$, where $R$ and $\sigma$ denote the rank and the signature (the sum of algebraic signs of the eigenvalues) of the Hessian matrix, respectively. These CPs can further be grouped into three sets, viz., (3,+3), (3,+1), and (3,−1). The (3,+3) CPs correspond to the local minima, whereas (3,+1) and (3,−1) correspond to the saddle points. These (3,+3) CPs represent potential binding sites for the electrophilic interactions.

## Results and Discussion

The optimized geometry of a glucose residue cut out of CD is shown in Figure 1 along with the atomic labels used. B3LYP/6-31G(d,p) optimized geometries of the α-, *β*-, and *γ*-CDs are

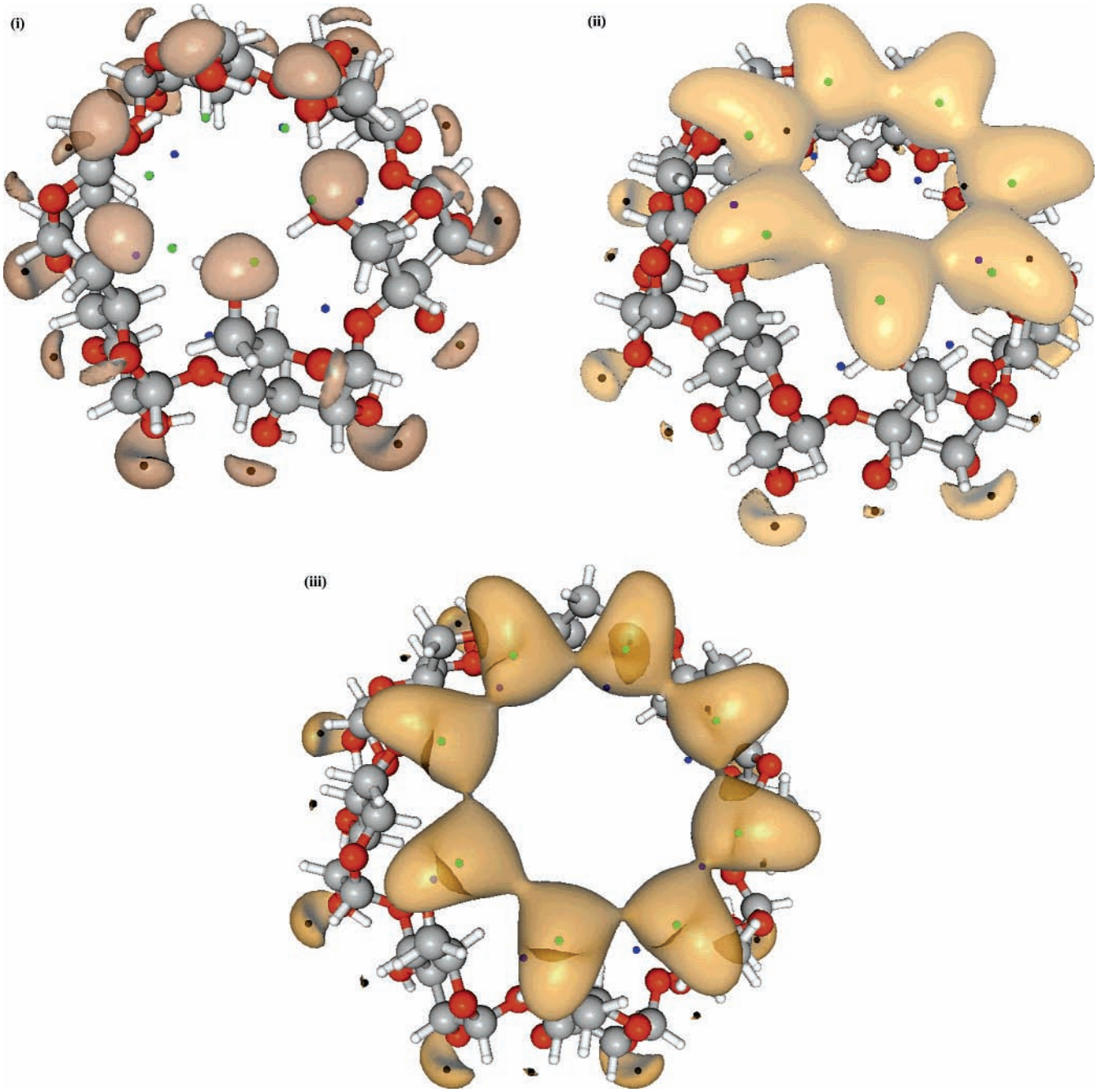


**Figure 4.** MESP isosurface ($V = -105$ kJ mol$^{-1}$) of (i) α-CD, (ii) $\beta$-CD, and (iii) $\gamma$-CD.

**TABLE 4: Cavity Diameter (Top and Bottom Rims) and Cavity Height (in Å) in α-, $\beta$-, and $\gamma$-Cyclodextrins**[a]

| | α-CD | $\beta$-CD | $\gamma$-CD |
|---|---|---|---|
| $d_w$ | 4.3 | 7.6 | 9.5 |
| $d_x$ | 6.6 | 7.6 | 9.5 |
| $d_{wx}$ | 3.1 | 3.4 | 3.2 |
| diameter[b] | 4.7−5.2 | 6−6.4 | 7.5−8.3 |

[a] $d_w$ and $d_x$, diameters of top and bottom rims; $d_{wx}$, height of cavity. See text for details. [b] The range of cavity diameters given in ref 60.

displayed in Figure 2. The input geometries of α-, $\beta$-, and $\gamma$-CDs subjected to the B3LYP optimizations are comprised of the hydrogen-bonded interactions between the primary (top rim) hydroxyls as well as those involving the secondary hydroxyl (bottom rim) groups, which are qualitatively similar. The single and double primes used hereafter refer to atoms from different (neighboring) glucoses. The optimized geometry of α-CD thus obtained shows that the $O_6-H\cdots O_6''$ interactions in the initial geometry are conserved. This engenders a cone-type structure. In $\beta$- and $\gamma$-CDs $O_5''\cdots H-O_6$ interactions prevail and a "barrel"-shaped structure has been predicted. B3LYP optimized geometric parameters of α-, $\beta$-, and $\gamma$-CDs are compared with those determined from X-ray crystal structures[27−28,58−60] in Table 1. Calculated average bond distances and bond angles in the glycosidic linkage and those in glucose units agree fairly well with their experimental counterparts. However, it should be noted here that the observed structures refer to the crystal data of hydrated CD whereas the calculated ones correspond to an isolated molecule in the gaseous state. The glycosidic $C_1O_4'$ bond distances (1.409 Å) in which $O_4$ does not participate in hydrogen bonding are unchanged in the α-, $\beta$-, and $\gamma$-CDs. Hydrogen-bonded interactions in primary −OH groups of α-CD

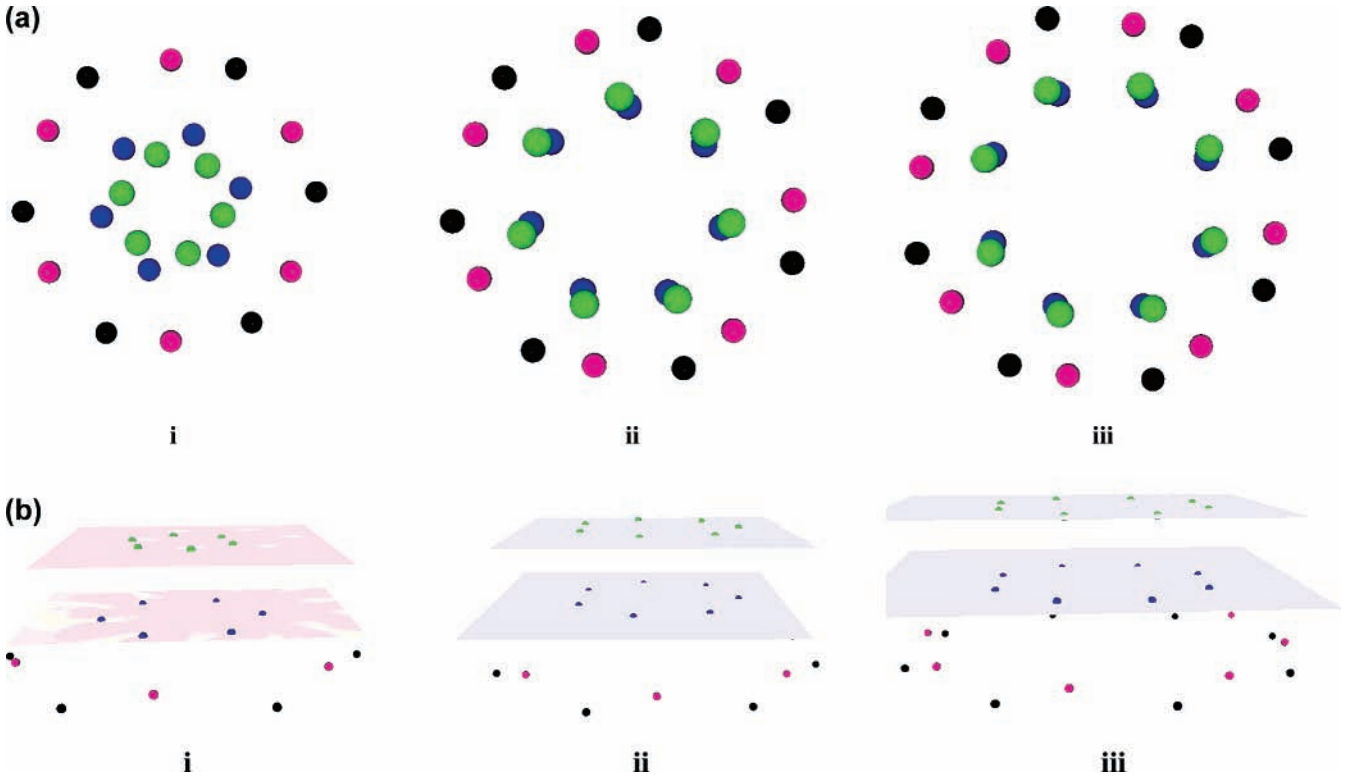


**Figure 5.** (a) Top view of array of CPs in MESP topography in (i) α-CD, (ii) $\beta$-CD, and (iii) $\gamma$-CD. (b) Lateral view of array of CPs w, x, y, and z in MESP topography in (i) α-CD, (ii) $\beta$-CD, and (iii) $\gamma$-CD. Planes defined by sets of w and x are shown. See text for details.

leads to a larger $O_6H$ bond distance (0.983 Å) compared to corresponding distances in $\beta$-CD and $\gamma$-CD (0.971 Å in both). On the other hand, $O_5''\cdots H-O_6$ hydrogen-bonded interactions in the $\beta$- and $\gamma$-CDs engender longer $C_1O_5$ and $C_5O_5$ bond distances.

The hydrogen-bonding pattern in α-, $\beta$-, and $\gamma$-CDs is shown in Figure 3. Owing to interactions in the secondary hydroxyl groups, the $C_2O_2$ bond length of α-CD turns out to be 0.005 Å longer than those in $\beta$- and $\gamma$-CDs. The strength of interactions in secondary hydroxyl groups in a glucose unit follows the rank order α-CD < $\beta$-CD < $\gamma$-CD. These are in accordance with the $O_3-H\cdots O_2$ bond distances reported in Table 2. The inter-glucose $O_2-H\cdots O_3'$ hydrogen-bonded interactions follow the same rank order as $O_3-H\cdots O_2$ interactions in glucose. As shown in Table 1, the $O_5-O_6$ and $O_4-O_6$ distances from the present calculations and those observed are different since the experimental data refer to the crystal structure whereas the calculated distances refer to the isolated molecule in the gas phase. The former interactions are, however, predicted to be relatively strong. Generally, most of the bond angles in glucoses differ by less than 2° in α-, $\beta$-, and $\gamma$-CDs. The larger cavity size of the $\gamma$-CD can be seen from the opening of a bond angle of glycosidic oxygens, i.e., $O_4O_4'O_4''$ from 120° in α-CD to 135° in $\gamma$-CD. A closure of the bridge angle $C_1O_4'C_4'$ on encompassing from α-CD to $\gamma$-CD has been noticed due to the release of strain with the increase in cavity size. As shown in Table 1, the $C_4C_5C_6O_6$ dihedral angle in α-CD is calculated to be −143° compared to −73° in $\beta$- or $\gamma$-CD. This large difference in the dihedral angle stems from the $O_6-H\cdots O_6''$ hydrogen-bonded interactions from the primary hydroxyl groups in α-CD. In $\beta$-CD as well as in $\gamma$-CD the $O_5''\cdots H-O_6$ interactions prevail and the $C_4C_5C_6O_6$ dihedral angle results in a barrel-type structure.

How the hydrogen-bonding patterns in the top and bottom rims of CD influence the overall dipole moment is intriguing. In this respect the conformers exhibiting either clockwise or counterclockwise hydrogen-bonded interactions in the top or the bottom rim of CD and the combinations thereof have been investigated by the semiempirical PM3 method. The following inferences may be drawn. (i) Both clockwise and counterclockwise hydrogen-bonding patterns in the top rim are present only in α-CD, and the dipole moments of these conformers are predicted to be nearly the same. (ii) Dipole moments of α-, $\beta$-, and $\gamma$-CDs are insensitive to the clockwise or counterclockwise hydrogen-bonding patterns in the bottom rim. In the framework of B3LYP theory, calculated dipole moments predict the rank order α-CD (1.6 D) < $\beta$-CD (7.2 D) < $\gamma$-CD (8.1 D), which agrees well with the conclusions drawn earlier. Thus, it may be inferred that the hydrophobic cavities of $\beta$- and $\gamma$-CDs are more polarized. As pointed out earlier, the MESP brings about the effective localization of electron-rich regions in the molecular system. The isosurface of $V = -105$ kJ mol$^{-1}$ is depicted in Figure 4 along with the (3,+3) CP in the electrostatic potential denoted by "w" (green), "x" (blue), "y" (black), and "z" (pink), representing minima near $O_6$ (primary hydroxyl), $O_4$ (glycosidic), and $O_2$, $O_3$ (both from the secondary hydroxyl group), respectively. From Figure 4 it is transparent that the electron-rich regions are projecting outward from the top rim in α-CD while in $\beta$- and $\gamma$-CDs these are pushing inside the cavity. This partly explains why α-CD favors interaction of the guest from the outside surface of the cavity while in $\beta$-CD the guest penetrates inside the cavity.[42]

MESP minima in the α-, $\beta$-, and $\gamma$-CDs defining different sets of CPs given by "w", "x", "y", and "z" are given in Table 3. As may be readily noticed, the minima near hydroxyl groups are deeper than those near glycosidic oxygens in $\beta$- and $\gamma$-CDs. In α-CD the minima of primary hydroxyl oxygens ("w") are shallow compared to those near the secondary hydroxyl oxygens ("y" and "z"). However, this is not found in $\beta$- or $\gamma$-CD. In other words, the inner cavity of α-CD is relatively less hydrophilic in nature. The deeper minima near $O_2$ than those

near $O_3$ (cf. Figure 4) suggest that the inter-glucose $O_2-H\cdots O_3'$ hydrogen-bonded interactions are stronger than the $O_3-H\cdots O_2$ interactions in the glucose unit of CD. This can also be inferred from the localized electron-rich regions near $O_2$ and $O_3$ in the MESP isosurface displayed in the figure. Thus, the strength of different hydrogen-bonded interactions can be gauged from the MESP topography.

As pointed out earlier, the MESP topography through its distributions of positive and negative potential regions provides insights for orientation of the guest molecules in the CD complexes. An average separation of radial opposite CPs yields a measure of the cavity diameter. Figure 5 shows an array of critical points "w", "x", "y", and "z" in the α-, *β*-, and *γ*-CDs. MESP minima are viewed from the top in Figure 5a, and a side view has been displayed in Figure 5b. For the sake of clarity the skeleton of CD is not shown. The "w" and "x" CPs in Figure 5a reveal a cone-like structure for the α-CD, while for *β*- and *γ*-CDs those yield a barrel-shaped structure. The plane containing CPs "w" and another one containing "x" are shown in Figure 5b, where the path joining "w" and "x" define the top rim and the bottom rim of the CD cavity. A separation of top and inner rims of the cavity has been estimated as follows. All the coordinates of CPs in the electrostatic potential are transformed to a new coordinate by setting of coordinates of "w" to zero by the appropriate rotational transformation. The plane containing critical points "x" is seen to be parallel to the earlier plane. Thus a separation of the two planes formed by "x" and "w" CPs yields the "cavity height" (cf. Table 4). The cavity dimensions of α-, *β*-, and *γ*-CDs are given in Table 4. Saenger[61] has reported the range for the cavity diameters from the distance between $H_5$ and $H_3$ hydrogen in CD. Effective cavity size diameters of the top and bottom rims calculated from the present work compare well with those reported in ref 60. Owing to a cone-like structure and relatively small diameter, α-CD can form a 2:1 inclusion complex with ferrocene whereas *β*- and *γ*-CDs are expected to yield 1:1 inclusion complexes, which has also been observed in the experiment.[62] The large cavity diameter of *γ*-CD allows the ferrocene molecule to interact along the diameter of the barrel in the inclusion complex with *γ*-CD.

In summary, the present work demonstrates how the MESP topography can be used to analyze hydrogen-bonded interactions and provides a measure for the effective cavity dimensions of α-, *β*-, and *γ*-CDs with consequent insights for the host−guest interactions.

## Conclusions

This work presents the electronic structure and the molecular electrostatic potential topography in α-, *β*-, and *γ*-CDs and shows how the MESP topography provides insights for CD complexation. Electrostatic potential investigations are used as the motif for hydrogen bonding in these molecular systems. In brief, the following conclusions may be drawn. The geometric parameters of the glycosidic linkage and those in glucose units of α-, *β*-, and *γ*-CDs from the B3LYP theory predict inter-glucose hydrogen bonds ($O_2-H\cdots O_3'$) to be relatively stronger than the intra-glucose $O_3-H\cdots O_2$ interactions. In α-CD the hydrogen bonding between primary hydroxyl groups ($O_6-H\cdots O_6''$) prevail. For *β*-CD and *γ*-CD the hydrogen-bonded interactions of ether oxygen in the glucose ring with primary hydroxyl group engender a "barrel-like" structure. MESP topography qualitatively explains the binding patterns of the guest molecule with the host, which can either interact externally as in α-CD or form inclusion complexes where the guest penetrates inside the cavity, which is observed in *β*- and *γ*-CDs. The orientation of the guest inside the CD cavity in the complex can be predicted a priori from the electrostatic potential investigations and the cavity dimensions. Estimates of cavity dimension partly explain the stoichiometry of inclusion complexes.

**Acknowledgment.** S.P.G. is grateful to the University Grants Commission (UGC), New Delhi, India, (Research Project No. F30-72/2004(SR)). R.V.P. and K.A.J. thank CSIR for a Research Fellowship. We thank Professor Rajeev K. Pathak for useful discussions.

## References and Notes

(1) Szejtli, J. *Chem. Rev.* **1998**, *98*, 1743.
(2) Connors, K. A. *Chem. Rev.* **1997**, *97*, 1325.
(3) Uekama, K. *J. Inclusion Phenom. Macrocycl. Chem.* **2002**, *44*, 3.
(4) Takahashi, K. *Chem. Rev.* **1998**, *98*, 2013.
(5) Kano, K.; Hasegawa, H. *J. Inclusion Phenom. Macrocycl. Chem.* **2001**, *41*, 41.
(6) (a) Buschmann, H. J.; Knittel, D.; Schollmeyer, E. *J. Inclusion Phenom. Macrocycl. Chem.* **2001**, *40*, 169. (b) Monti, S.; Sortino, S. *Chem. Soc. Rev.* **2002**, *31*, 287. (c) Harada, A. *Acc. Chem. Res.* **2001**, *34*, 456.
(7) Guillaume, Y. C.; Guinchard, C. *J. Phys. Chem. B* **1997**, *101*, 8390.
(8) Song, L.; Purdy, W. C. *Chem. Rev.* **1992**, *92*, 1457.
(9) Tomasella, F. P.; Zuting, P.; Cline Love, L. J. *Supramol. Chem.* **1992**, *1*, 25.
(10) Uekama, K. *Chem. Pharm. Bull.* **2004**, *52*, 9000.
(11) Kopecky, F.; Vojtekova, M.; Kaclik, P.; Demko, M.; Bielikova, Z. *J. Pharm. Pharmacol.* **2004**, *56*, 581.
(12) Strickley, R. G. *Pharm. Res.* **2004**, *21*, 201.
(13) Mora, P. C.; Cirri, M.; Allolio, B.; Carli, F.; Mura, P. *J. Pharm. Sci.* **2003**, *92*, 2177.
(14) Chourasia, M. K.; Jain, S. K. *J. Pharm. Pharm. Sci.* **2003**, *6*, 33.
(15) Li, J.; Ni, X. P.; Leong, K. W. *J. Biomed. Mater. Res. A* **2003**, *65*, 196.
(16) Loftsson, T.; Brewster, M. E. *J. Pharm. Sci.* **1996**, *85*, 1017.
(17) Thompson, D. O. *Crit. Rev. Ther. Drug Carrier Syst.* **1997**, *14*, 1.
(18) Uekama, K.; Hirayama, F.; Irie, T. *Chem. Rev.* **1998**, *98*, 2045.
(19) (a) Breslow, R.; Dong, S. D. *Chem. Rev.* **1998**, *98*, 1829. (b) Cao, F.; Ren, Y.; Hua, W.-Y.; Ma, K.-F.; Guo, Y.-L. *Chin. J. Org. Chem.* **2002**, *22*, 827.
(20) Abreu, A. R.; Costa, I.; Rosa, C.; Ferreira, L. M.; Lourenço, A.; Santos, P. P. *Tetrahedron* **2005**, *61*, 11986.
(21) Wenz, G. *Angew. Chem., Int. Ed. Engl.* **1994**, *33*, 803.
(22) Engeldinger, E.; Armspach, D.; Matt, D. *Chem. Rev.* **2003**, *103*, 4147.
(23) Schneider, H.-J.; Hacket, F.; Rüdiger, V. *Chem. Rev.* **1998**, *98*, 1755.
(24) Puliti, R.; Mattia, C. A.; Paduano, L. *Carbohydr. Res.* **1998**, *310*, 1.
(25) Fujiwara, T.; Tanaka, N.; Kobayashi, S. *Chem. Lett.* **1990**, 739.
(26) Jacob, J.; Gessler, K.; Hoffmann, D.; Sanbe, H.; Koizumi, K.; Smith, S. M.; Takaha, T.; Saenger, W. *Angew. Chem., Int. Ed.* **1998**, *37*, 606.
(27) Harata, K. *Bull. Chem. Jpn.* **1987**, *60*, 2763.
(28) Chacko, K. K.; Saenger, W. *J. Am. Chem. Soc.* **1981**, *103*, 1708.
(29) (a) Luo, L. B.; Chen, H. U.; Tang, W. X.; Zang, Z. Y.; Mark, T. C. W. *J. Chem. Soc., Dalton Trans.* **1996**, 4425. (b) Saenger, W.; Steiner, T. *Acta Crystallogr., Sect. A* **1998**, *54*, 798. (c) Harata, K. In *Inclusion Compounds*; Atwood, J. L.; Davies, J. E. D., MacNicol, D. D., Eds.; Academic Press: London, 1991; Vol. 5, pp 311−344. (d) Klar, B.; Hingerty, B.; Saenger, W. *Acta Crystallogr., Sect. B* **1980**, *36*, 1154. (e) Manor, P. C.; Saenger, W. *J. Am. Chem. Soc.* **1974**, *96*, 3630. (f) Lindner, K.; Saenger, W. *Acta Crystallogr., Sect. B* **1982**, *38*, 203. (g) Betzel, Ch.; Saenger, W.; Hingerty, B.; Brown, G. M. *J. Am. Chem. Soc.* **1984**, *106*, 7545. (h) Ding, J.; Steiner, T.; Zabel, V.; Hingerty, B. E.; Mason, S. A.; Saenger, W. *J. Am. Chem. Soc.* **1991**, *113*, 8081. (i) Zabel, V.; Saenger, W.; Mason, S. A. *J. Am. Chem. Soc.* **1986**, *108*, 3664.
(30) Lima, S.; Goodfellow, B. J.; Teixeira-Dias, J. J. C. *J. Phys. Chem. B* **2003**, *107*, 14590.
(31) Cunha-Silva, L.; Teixeira-Dias, J. J. C. *New J. Chem.* **2004**, *28*, 200.
(32) (a) Ortona, O.; Paduano, L.; Costantino, L.; Vitagliano, V. *J. Mol. Liq.* **1995**, *63*, 291. (b) Ciccarelli, D.; Paduano, L.; Costantino, L.; Ortona, O.; Vitagliano, V. *J. Mol. Liq.* **1998**, *75*, 169.
(33) (a) Saenger, W.; Beyer, K.; Manor, P. C. *Acta Crystallogr., Sect. B* **1976**, *32*, 120. (b) Harata, K. *Bull. Chem. Soc. Jpn.* **1979**, *52*, 2451.
(34) Anslyn, E. V.; Dougherty, D. D. *Modern Physical Organic Chemistry*; University Science Books: Sausalito, California, 2005; p 234.
(35) Tran, C. D.; De Paoli Lacerda, S. H. *Anal. Chem.* **2002**, *74*, 5337.

(36) Godýnez, L. A.; Schwartz, L.; Criss, C. M.; Kaifer, A. E. *J. Phys. Chem. B* **1997**, *101*, 3376.

(37) Lipkowitz, K. B. *Chem. Rev.* **1998**, *98*, 1829.

(38) (a) Bonnet, P.; Jaime, C.; Morin-Allory, L. *J. Org. Chem.* **2001**, *66*, 689. (b) Barbiric, D. J.; De Rossi, R. H.; Castro, E. A. *THEOCHEM* **2001**, *537*, 235. (c) Oana, M.; Tintaru, A.; Gavriliu, D.; Maior, O.; Hillebrand, M. *J. Phys. Chem. B* **2002**, *106*, 257. (d) Pastor, I.; Di Marino, A.; Mendicuti, F. *J. Phys. Chem. B* **2002**, *106*, 1995. (e) Cunha-Silva, L.; Teixeira-Dias, J. J. C. *J. Inclusion Phenom. Macrocycl. Chem.* **2002**, *43*, 127.

(39) Lukovits, I. *J. Mol. Struct. (THEOCHEM)* **1988**, *170*, 249.

(40) Rekharsky, M. V.; Mayhew, M. P.; Goldberg, R. N.; Ross, P. D.; Yamashoji, Y.; Inoue, Y. *J. Phys. Chem. B* **1997**, *101*, 87.

(41) (a) Nie, M.-Y.; Zhou, L.-M.; Wang, Q.-H.; Zhu, D.-Q. *Acta Chim. Sin.* **2001**, *59*, 268. (b) Varady, J.; Wu, X.; Wang, S. *J. Phys. Chem. B* **2002**, *106*, 4863. (c) Bonnet, P.; Jaime, C.; Morin-Allory, L. *J. Org. Chem.* **2002**, *67*, 8602. (d) Bea, I.; Jaime, C.; Kollman, P. *Theor. Chem. Acc.* **2002**, *108*, 286. (e) Lawtrakul, L.; Viernstein, H.; Wolschann, P. *Int. J. Pharm.* **2003**, *256*, 33. (f) Yin, K.-L.; Xu, D.-J.; Chen, C.-L. *Acta Phys. Chim. Sin.* **2003**, *19*, 480. (g) Mele, A.; Raffaini, G.; Ganazzoli, F.; Selva, A. *J. Inclusion Phenom. Macrocycl. Chem.* **2002**, *44*, 219. (h) Reddy, M. N.; Rehana T.; Ramakrishna, S.; Chowdary, K. P. R.; Diwan, P. V. *AAPS PharmSci* **2004**, *6*, 1.

(42) Estrada, E.; Perdomo-López, I.; Torres-Labandeira, J. J. *J. Chem. Inf. Comput. Sci.* **2001**, *41*, 1561.

(43) Winklera, R. G.; Fioravantia, S.; Ciccottib, G.; Margheritisc, C.; Villa, M. *J. Comput.-Aided Mol. Des.* **2000**, *14*, 659.

(44) Liu, L.; Li, X.-S.; Guo, Q.-X. *J. Mol. Struct. (THEOCHEM)* **2000**, *530*, 31.

(45) Hobza, P.; Zahrdnik, R. *Collect. Czech. Chem. Commun.* **1974**, *39*, 2857.

(46) Dos Santos, H. F.; Duarte, H. A.; Sinisterra, R. D.; De Melo Mattos, S. V.; De Oliveira, L. F. C.; De Almeida, W. B. *Chem. Phys. Lett.* **2000**, *319*, 569.

(47) Nascimento, C. S., Jr.; Dos Santos, H. F.; De Almeida, W. B. *Chem. Phys. Lett.* **2004**, *397*, 422.

(48) Nascimento, C. S., Jr.; Cleber, P. A.; Dos Santos, H. F.; De Almeida, W. B. *J. Phys. Chem. A* **2005**, *109*, 3209.

(49) Li, X.-S.; Liu, L.; Mu, T.-W.; Guo, Q.-X. *Monatsh. Chem.* **2000**, *131*, 849.

(50) Madrid, J. M.; Mendicuti, F.; Mattice, W. L. *J. Phys. Chem. B* **1998**, *102*, 2037.

(51) Matsushita, Y.; Suzuki, T.; Ichimura, T.; Hikida, T. *J. Phys. Chem. A* **2004**, *108*, 7490.

(52) Becke, D. *J. Chem. Phys.* **1993**, *98*, 5684.

(53) Lee, C.; Yang, W.; Parr, R. G. *Phys. Rev. B* **1988**, *37*, 785.

(54) Frisch, M. J.; Trucks, G. W.; Schlegel, H. B.; Scuseria, G. E.; Robb, M. A.; Cheeseman, J. R.; Montgomery, J. A.; Vreven, T., Jr.; Kudin, K. N.; Burant, J. C.; Millam, J. M.; Iyengar, S. S.; Tomasi, J.; Barone, V.; Mennucci, B.; Cossi, M.; Scalmani, G.; Rega, N.; Petersson, G. A.; Nakatsuji, H.; Hada, M.; Ehara, M.; Toyota, K.; Fukuda, R.; Hasegawa, J.; Ishida, M.; Nakajima, T.; Honda, Y.; Kitao, O.; Nakai, H.; Klene, M.; Li, X.; Knox, J. E.; Hratchian, H. P.; Cross, J. B.; Adamo, C.; Jaramillo, J.; Gomperts, R.; Stratmann, R. E.; Yazyev, O.; Austin, A. J.; Cammi, R.; Pomelli, C.; Ochterski, J. W.; Ayala, P. Y.; Morokuma, K.; Voth, G. A.; Salvador, P.; Dannenberg, J. J.; Zakrzewski, V. G.; Dapprich, S.; Daniels, A. D.; Strain, M. C.; Farkas, O.; Malick, D. K.; Rabuck, A. D.; Raghavachari, K.; Foresman, J. B.; Ortiz, J. V.; Cui, Q.; Baboul, A. G.; Clifford, S.; Cioslowski, J.; Stefanov, B. B.; Liu, G.; Liashenko, A.; Piskorz, P.; Komaromi, I.; Martin, R. L.; Fox, D. J.; Keith, T.; Al-Laham, M. A.; Peng, C. Y.; Nanayakkara, A.; Challacombe, M.; Gill, P. M. W.; Johnson, B.; Chen, W.; Wong, M. W.; Gonzalez, C.; Pople, J. A. *Gaussian 03*; Gaussian Inc.: Wallingford, CT, 2004.

(55) Gadre, S. R.; Bhadane, P. K.; Pundlik, S. S.; Pingale, S. S. *Molecular Electrostatic Potentials: Concepts and Applications*; Murray, J. S., Sen, K. D., Eds.; Elsevier: Amsterdam, 1996.

(56) Limaye, A. C.; Gadre, S. R. *Curr. Sci.* **2001**, *80*, 1298.

(57) Balanarayan, P.; Gadre, S. R. *J. Chem. Phys.* **2003**, *119*, 5037.

(58) Saenger, W.; Jacob, J.; Gessler, K.; Steiner, T.; Hoffmann, D.; Sanbe, H.; Koizumi, K.; Smith, S. M.; Takaha, T. *Chem. Rev.* **1998**, *98*, 1787.

(59) Bakó, I.; Jicsinszky, L. *J. Inclusion Phenom. Mol. Recognit. Chem.* **1994**, *18*, 275.

(60) Lindner, K.; Saenger, W. *Carbohydr. Res.* **1982**, *99*, 103.

(61) Saenger, W. *Angew. Chem., Int. Ed. Engl.* **1980**, *19*, 344.

(62) (a) Harada, A.; Takahashi, S. *J. Inclusion Phenom.* **1984**, *2*, 791. (b) Harada, A.; Takahashi, S. *Chem. Lett.* **1984**, 2089. (c) Harada, A.; Hu, Y.; Yamamoto, S.; Takahashi, S. *J. Chem. Soc., Dalton Trans.* **1988**, 729. (d) Hapiot, F.; Tilloy, S.; Monflier, E. *Chem. Rev.* **2006**, *106*, 767.